Study the effect of MRF Model based NC classifier with different distance measures and parameters

Shilpa Suman[1*], Anil Kumar[2], Dheeraj Kumar[1]

[1]Remote sensing and GIS laboratory, Department of Mining Engineering, Indian Institute of Technology (Indian School of Mines), Dhanbad 826004, India (dheeraj@iit.ism.ac.in)
[2]Indian Institute of Remote Sensing (IIRS), Dehradun 248001, India (anil@iirs.gov.in)
*Email: shilpa.suman011@gmail.com

(Received: 26 August 2022, Accepted in final form: 11 November 2022)

DOI- *https://doi.org/10.58825/jog.2023.17.1.79*

Abstract: The accuracy of satellite image classification and the computational complexity is reduced due to the image's noisy pixels. Therefore, spatial contextual information-based classifiers are required to handle the noisy pixels and obtain the neighborhood information. This paper represents Noise clustering (NC) based Markov Random Field (MRF) models (SP, DA (H1, H2, H3, and H4)) that handle the noisy pixels and provide the information. The Smoothing Prior (SP) and Discontinuity Adaptive (DA) models are useful for reducing noise by smoothing the images and showing the boundary of classes, respectively. This study has carried out a comparative study among MRF model-based NC classifiers SP and DA for different distance measures and parameters. MRF models based on NC classifiers were tested for classifying Eucalyptus, Water, Riverine sand, Grassland, Dense Forest, and Wheat classes using the Formosat-2 and Landsat-8 multispectral images of the Haridwar area. The DA (H1) model provides the best overall accuracy (85.09%) for m=1.3, λ=0.2, $\delta=10^4$,γ=0.8, and Mean Absolute Difference.

Keywords: NC, MRF, DA, SP, Distance Measures

1. Introduction

A hard/conventional classification technique does not look after the neighborhood pixel and noisy pixel information of land cover classes. The neighborhood, noisy and mixed pixels are essential in the gradual boundary change problem. To incorporate this problem, many researchers implemented the "Soft Classification" approach; these techniques follow fuzzy logic theory and the fuzzy set applied to handle the problem of noisy and mixed pixels (Fisher 1997). The occurrence of noisy pixels degrades the accuracy of image classification (Singh and Garg 2017). The fuzzy based-approach allocates individual pixels to one or more classes. Fuzzy classification is also known as the soft classification technique (Binaghi and Rampini 1993). Fuzzy classification is illustrated by Possibilistic c-means (PCM) (Krishnapuram and Keller 1993), Fuzzy c-means (FCM) (Bezdek et.al, 1984), and Noise Clustering (NC) (Dave and Krishnapuram 1997). This paper concentrates on NC classifiers proposed by Dave R. N. (1991) to handle the sensitivity of the FCM algorithm from noisy and outlier pixels. The NC classifier introduced the additional cluster that is supposed to contain all outliers. This classifier minimizes the noise and outliers but does not give spatial contextual information. This information provides the neighboring pixel relationship, which helps handle mixed and noisy pixels and offers good accuracy results. The spatial context represents the relation between the adjacent pixels.

In order to extract the neighborhood pixel information and handle the noisy pixel, MRF models were introduced in the NC classifier, which is a visionary approach to considering spatial contextual information (Geman and Geman 1984). MRF models were initially introduced for computer vision, image processing, and statistical physics; recently, this model has been applied to classify and interpret remote sensing images (Zhang et al. 2011). MRF model considers the spatial attraction among pixels in the images. The property of contextual information is implemented using Smoothness Priors (SP). It smooths the images to reduce the noise, but it does not take about the edges or boundaries of classes in the smoothing process (Li 1995). DA model overcomes the problem of over-smoothing and is used for edge enhancement (Li 1995). Various applications need of MRF model to distinctly extract the information. Solberg et al. (1996) used the MRF model to classify the satellite images, and it was observed that the MRF model obtained 2% higher classification accuracy. Tso and Olsen (2005) analyzed that the MRF method increased classification accuracy as well as visual interpretation. Zhang et al. (2011) reported that MRF based model improved the classification accuracy. To increase the overall accuracy and reduce the noisy data and outliers, this paper studies the outcome of the MRF model-based NC classifier concerning various distance measures and different parameters. This optimized algorithm may be used to create a land use land cover map that can be used in integration with hazard maps to prepare a risk map for the desired area, agricultural mapping, and other fields that require a highly accurate LULC map (Rawat et al. 2022a; Saha et. al, 2022; Rawat et al. 2022b; Suman et.al, 2022)

The aims of this study show how different parameters (fuzziness factor (m), beta (β), lambda (λ), and gamma (γ)) and distance measures affect the MRF model with NC as the basic classifier. This study gives the optimized algorithm concerning different distance measures and parameters that handle the noisy data and enhance accuracy. A fuzzy Error Matrix (FERM) (Binaghi et al. 1999) has been implemented in this paper to obtain the overall accuracy of the classified output.

2. Mathematical details of NC and MRF Model

2.1. Noise Clustering

Noise clustering classifiers introduced a new cluster to contain all outliers to increase the accuracy (Davé and Krishnapuram 1997). Noise distance (δ) has an essential role in selecting which membership values lie on the new clusters. The NC algorithm objective function was given in eq. (1):

$$J_m = \sum_{i=1}^{N}\sum_{k=1}^{C} u_{ki}^{m}\|x_i - v_k\|^2 + \sum_{i=1}^{N}\delta^2\left(1 - \sum_{k=1}^{C} u_{ki}\right)^m \quad (1)$$

The membership value, mean value, and noise distance were obtained from eq. (2), eq. (3), and eq. (4) respectively, and updated this equation in equation 1 to get the objective function of the NC classifier.

$$u_{ki} = \frac{1}{\sum_{j=1}^{c}\left[\frac{\|x_i - v_k\|^2}{\|x_i - v_j\|^2}\right]^{\frac{1}{m-1}} + \left[\frac{\|x_i - v_k\|^2}{\delta^2}\right]^{\frac{1}{m-1}}} \quad (2)$$

$$v_k = \frac{\sum_{k=1}^{N}(u_{ki})^m x_i}{\sum_{k=1}^{N}(u_{ki})^m} \quad (3)$$

$$\delta^2 = \lambda\left[\frac{\sum_{k=1}^{C-1}\sum_{i=1}^{N}\|x_i - v_k\|^2}{n(c-1)}\right] \quad (4)$$

Here, u_{ki}= Degree of membership represents of ith pixel for cluster k,x_i= ith d-dimensional measured data,v_k= mean value (cluster center) of the kth class, m = Fuzziness factor (with a real value greater than one), N = total no of a pixel in the image, v_j= mean value (cluster center) of the jth class, C =Number of classes, δ= Noise Distance,$\|x_i - v_k\|$= distance betweenx_i and $v_k$and $\|x_i - v_j\|$= distance between x_i and v_j .

2.2. Discontinuity Adaptive (DA)

Discontinuity Adaptive (DA) is an important technique in the MRF model. This model conserves the edges and boundaries of classes. The required condition for a regulizer to be DA is defined in eq. (5) (Smits and Dellepiane 1997).

$$\lim_{n\to\infty}|g'(\eta)| = \lim_{n\to\infty}|2\eta h(\eta)| = c \quad (5)$$

c = constant (cε[0,∞])

The DA model (H1, H2, H3, and H4) is shown in eqs. (6-9).

$$g_{1\gamma}(\eta) = -\gamma e^{\frac{\eta^2}{\gamma}} \quad (6)$$

$$g_{2\gamma}(\eta) = \frac{-\gamma}{1+\frac{\eta^2}{\gamma}} \quad (7)$$

$$g_{3\gamma}(\eta) = \gamma \ln\left(1 + \frac{\eta^2}{\gamma}\right) \quad (8)$$

$$g_{4\gamma}(\eta) = \gamma|\eta| - \gamma^2 \ln\left(1 + \frac{|\eta|}{\gamma}\right) \quad (9)$$

2.3. Smoothing Prior (SP)

The MRF Smoothing Prior (SP) gives context information. It provides the concerned pixel as well as neighboring pixel information. A prior probability mathematically gave the smoothness assumption in the form of energy (Li 1995). For representing the prior energy, an analytical regulizer is implied. The basic structure of the regulizer is given in eqs. (10).

$$U(F) = \sum_{n=1}^{N} U_n(f) = \sum_{n=1}^{N} \lambda_n \int_n^b g(f^n(x))dx \quad (10)$$

U(f) = prior energy, represents the n^{th} order regularizer, λ_n=weighting factor, where(λ_n>=0) and$g(f^n(x))$ =potential function.

$$g(f^n(x)) = g(n) = \eta^2 \quad (11)$$

3. Study Area and Dataset Used

The study area (Figure 1.) for this research was the Haridwar district in the Indian state of Uttarakhand. This study lies between latitudes 29°49'14" and 29°52'21" and longitudes 78°9'17" and 78°13'4". The coverage area is 5.92×5.95 km^2, north to south and east to west. This study area mainly contains Eucalyptus, Riverine sand, Water, Grassland, Dense Forest, and Wheat to examine the different fuzzy classifier methods. Table 1. shows the specification of Landsat-8 and Formosat-2 sensors used in this study

.

Table 1. Specification of Landsat-8 and Formosat2 sensors

Specification	Landsat-8	Formosat-2
Spatial Resolution (m)	30 m	8 m
Spectral Resolution (μm)	B1: 0.450-0.515 μm (Blue) B2: 0.525-0.600 μm (Green) B3: 0.630-0.680 μm (Red) B4: 0.845-0.885 μm (Near Infrared)	B1: 0.45-0.52 μm (Blue) B2: 0.52-0.60 μm (Green) B3: 0.63-0.69 μm (Red) B4: 0.76-0.90 μm (Near Infrared)
Revisit Period	Repeat every 16 days	Daily

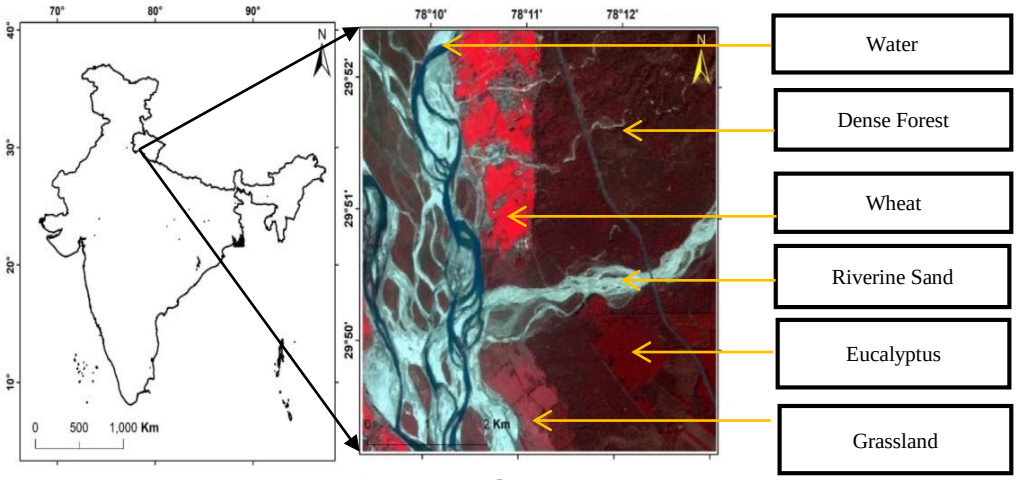

Figure 1. Study Area

4. Methodology Adopted

Figure 2 shows the methodology used for this study. This research focused on studying the effect of various parameters and distance measures by applying the NC as base classifiers for the MRF model. NC was used as the base classifier for MRF models, including contextual and spatial information (SP and DA (H1, H2, H3, and H4). The fraction output images from Landsat-8 and Formosat-2 were classified, and reference datasets were created. Various parameters were employed in this study, including λ (0.2-0.9) and γ (0.1-9) with a period of 0.1, m (1.1-3), and β (1-9) with intervals of 0.2 and 1, respectively. In the SP algorithm, the γ and m parameters were used, whereas, in the DA algorithm, β and m parameters were used. Mean Absolute Difference (Vassiliadis et al. 1998), Median Absolute Difference (Scollar et al, 1984), Normalized Square Euclidean (Hasnat et al. 2013), Canberra(Agarwal et.al, 2009), Manhattan (Hasnat et al. 2013), Chessboard (Baccour and John 2014) and Braycurtis (Bray and Curtis 1957), Cosine (Senoussaoui et al. 2014), Correlation (Székely et. al, 2007), and Euclidean (Baccour and John 2014) are different distance measures.

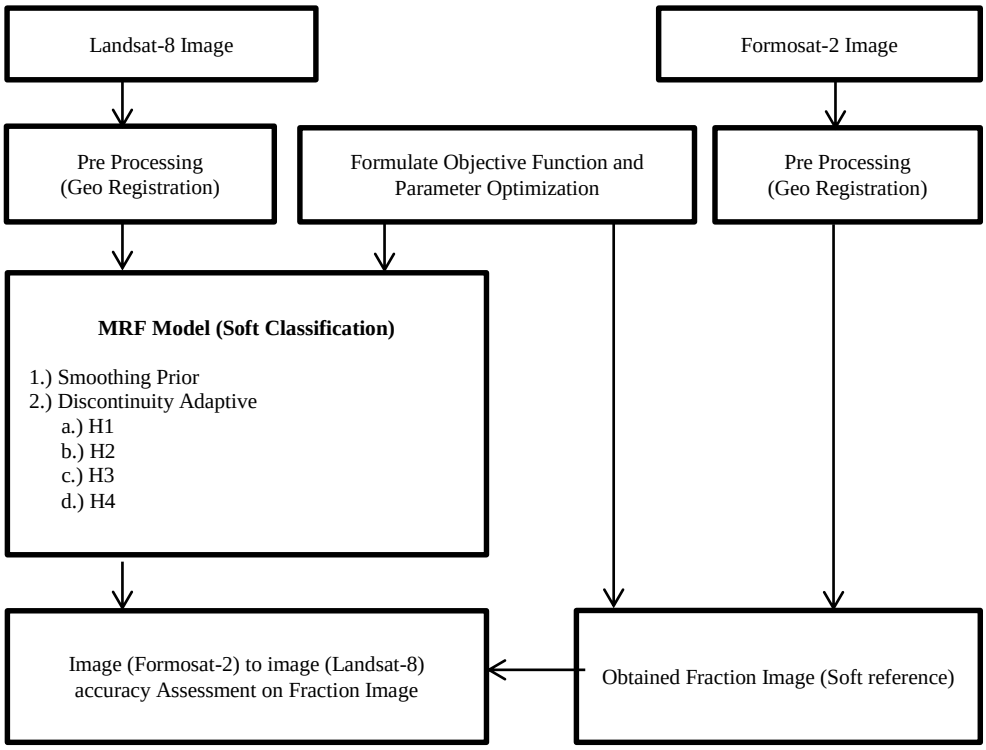

Figure 2. Methodology Adopted

The following steps show the adopted methodology.

Step 1: The satellite images were classified using the MRF model, which used NC as the base classifier for various parameters and distance measures, with m=1.1 and $\delta=10^4$.
Step 2: The optimized parameters have been obtained for the classified images' overall accuracy (OA).
Step 3: Obtained optimum parameters and different m values between 1.1 and 3 with a period of 0.2 were applied to classify the MRF model with NC as the base classifier.
Step 4: Finally, the Accuracy Assessment optimized the approach for various distance measures and parameters.

5. Results and Discussion

In this research, results were divided mainly into two parts. In the first part, the optimized parameter was obtained for SP and DA. The second part used optimized parameters to obtain the optimized MRF model technique, where NC was applied as the base classifier. The graph was built between parameters (λ, γ, β) and Overall Accuracy (OA) for various distance measures.

Figure 3 shows the DA (H1) (Figure 3(a-h)) and DA (H2) (Figure 3 (i–p)) algorithm applying NC as base classifier overall accuracy concerning γ and distance measures for the various value of λ (0.2-0.9) with an interval of 0.1

Table 2 represents the interpretation of Figure 3. It shows maximum overall accuracy for H1 and H2 using NC as the base classifier for the combination of distance measures and γ for different values of λ where m=1.1.

Figure 4 depicts the DA (H3) (Figure 4 (a-h)) and DA (H4) (Figure 4 (i–p)) algorithms for overall accuracy with regard to γ and distance measures for various values of (0.2-0.9) with an interval of 0.1 applying NC as a base classifier.

Table 3 obtains the analysis of Figure 4. It represents maximum overall accuracy for H3 and H4 using NC as the base algorithm for the combination of distance measures and γ for the various value of λ where m=1.1

Figure 5 represents the SP algorithm using NC as a base classifier for overall accuracy concerning γ and distance measures for the various value of λ (0.2-0.9) with an interval of 0.1

Table 4 represents the interpretation of Figure 5. It shows maximum overall accuracy for SP using NC as the base classifier for the combination of distance measures and γ for different values of λ where m=1.1.

Table 5 shows the highest overall accuracy of SP and DA (H1, H2, H3, H4) for various parameters (λ, γand β) and distance measurements where 'm'=1.1 using the basic classifier NC. Figure 6 was created using several distance measures between m and overall accuracy (OA), applying optimized parameters obtained from Table 5. Figure 6 depicts the NC, DA, and SP algorithms, with NC acting as the basic classifier for determining the optimal approach for different distance measures and m values.

Table 6 represents the inference of Figure 6. It shows the highest OA occurred for NC and NC based MRF model for different m value and distance measures.

Table 7 represents the maximum overall accuracy obtained from the various algorithms (DA (H1, H2, H3, and H4), SP, and NC) for m value and distance measures.

Table 2. Maximum overall accuracy for H1 and H2 using NC as a base classifier for the combination of distance measures and γ for different values of λ where m=1.1

	DA(H1)			DA(H2)		
λ	γ	Overall Accuracy (OA)	Distance Measures	γ	Overall Accuracy (OA)	Distance Measures
0.2	0.8	84.93	Mean Absolute Difference	0.8	1.79	Canberra
0.3	0.7	83.88	Canberra	0.9	1.86	Bray-Curtis
0.4	0.7	83.22	Bray-Curtis	0.9	16.92	Chessboard
0.5	0.7	82.51	Mean Absolute Difference	0.9	24.66	Chessboard
0.6	0.8	83.12	Mean Absolute Difference	0.9	49.26	Canberra
0.7	0.7	82.52	Canberra	0.9	63.98	Chessboard
0.8	0.8	83.58	Mean Absolute Difference	0.8	69.94	Mean Absolute Difference
0.9	0.7	84.32	Mean Absolute Difference	0.8	79.58	Bray-Curtis

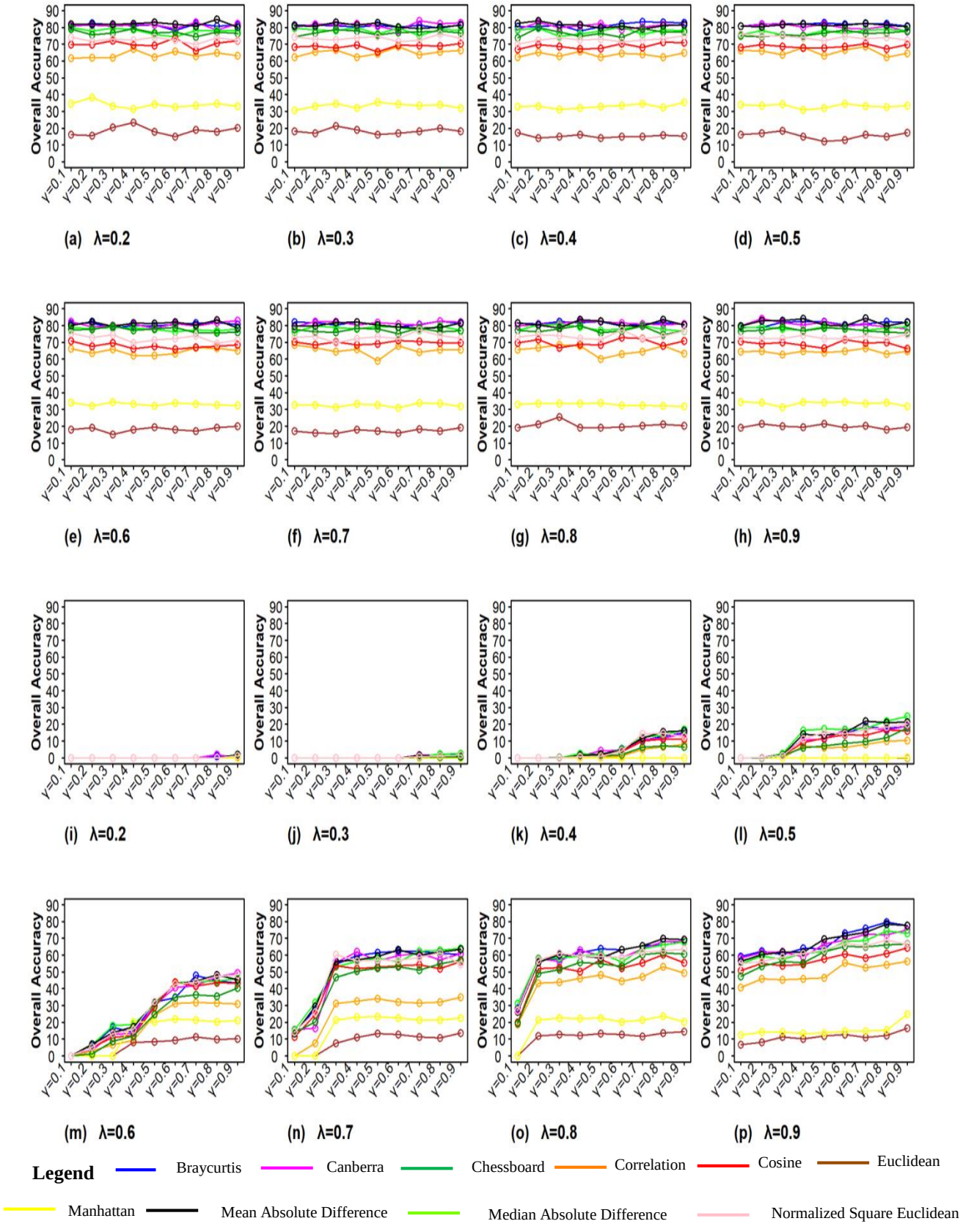

Figure 3. Comparison of Overall Accuracy in Discontinuity Adaptive Prior (DA) (H1) figure 3 (a-h) where DA (H2) figure 3 (i-p) using base classifier NC for applying different distance measures and m=1.1

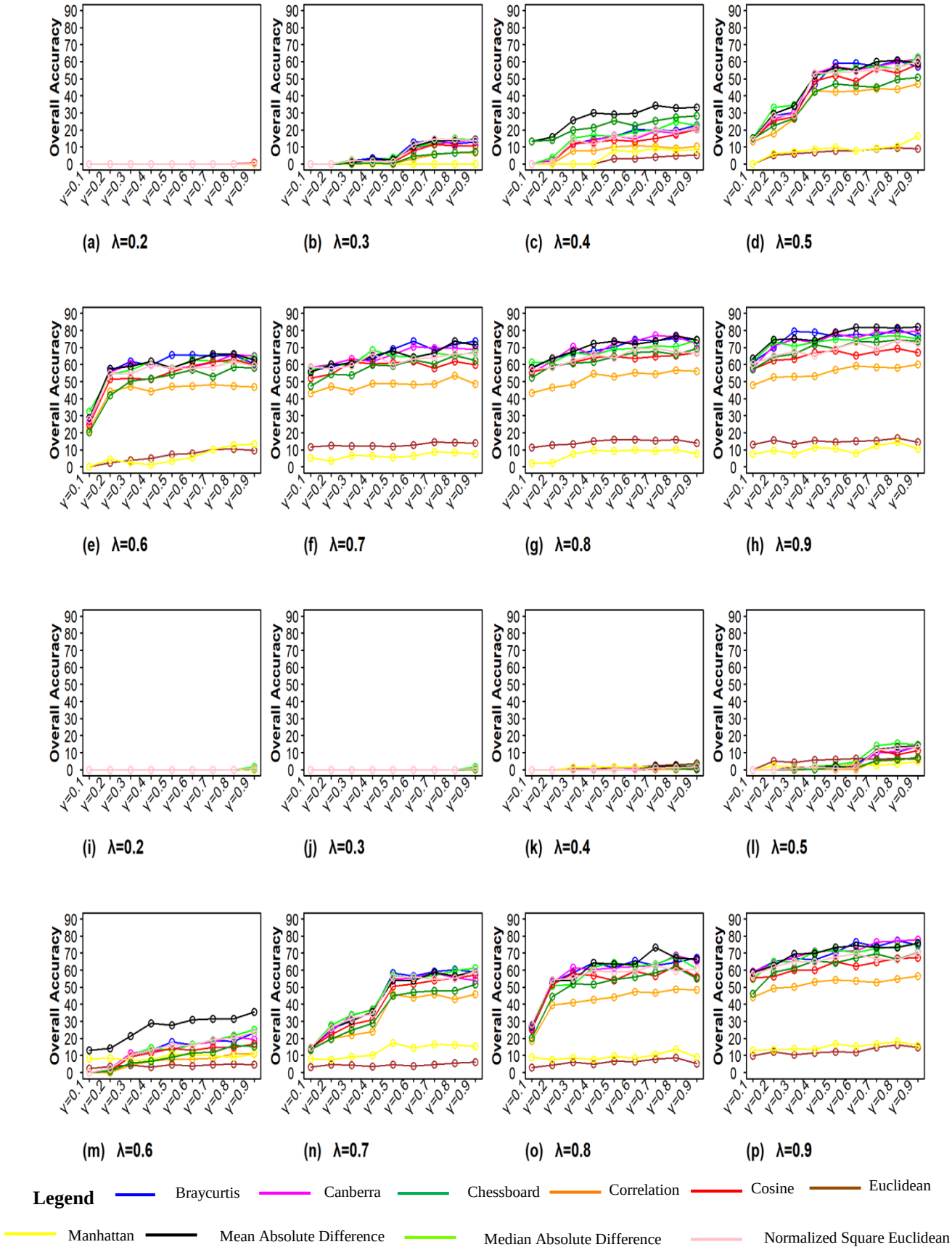

Figure 4. Comparison of Overall Accuracy in Discontinuity Adaptive Prior (DA) (H3) figure 4 (a-h) where DA (H4) figure 4 (i-p) using base classifier NC for applying different distance measures and m=1.1

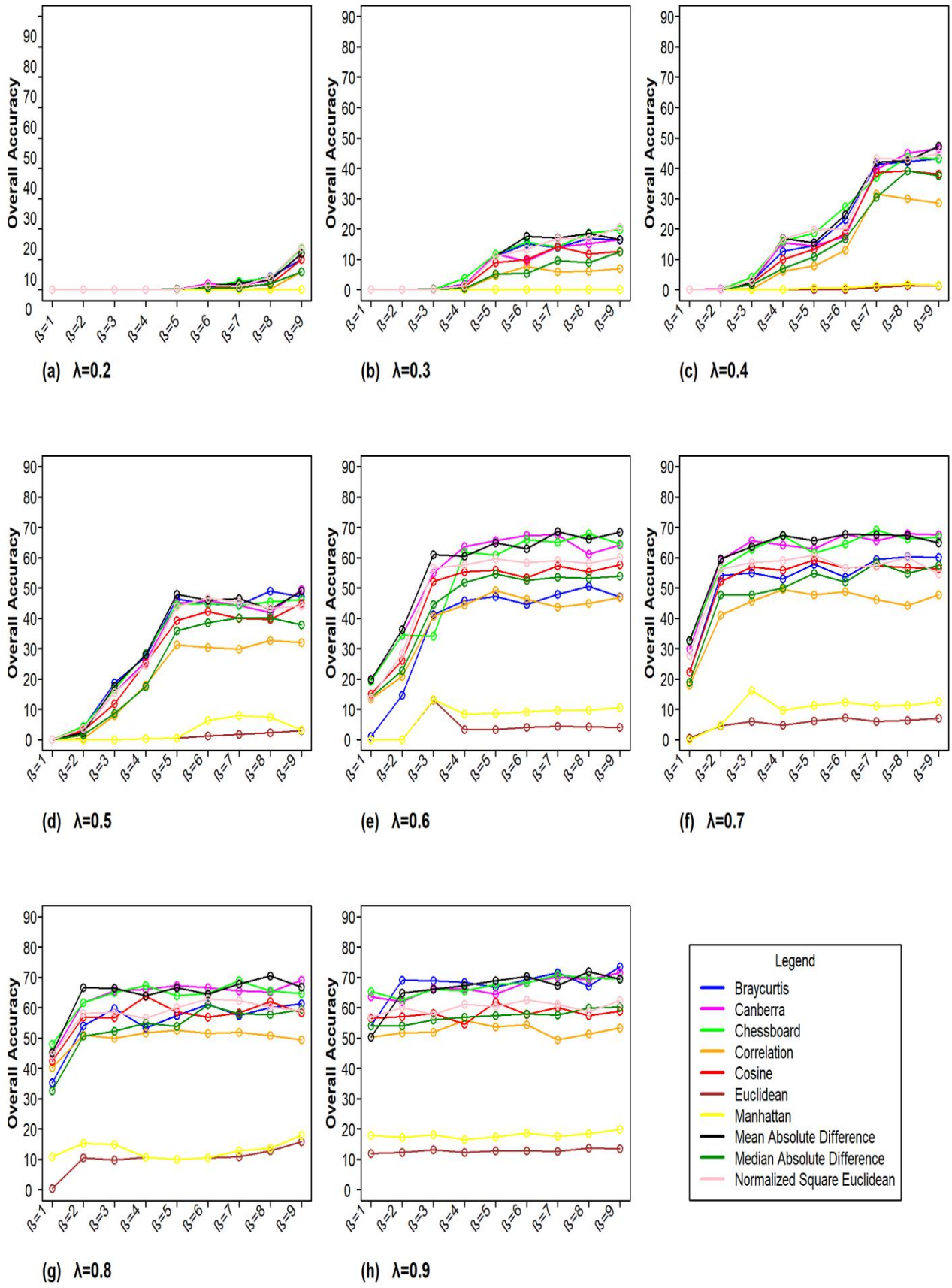

Figure 5. Comparison of Overall Accuracy in Smoothing Prior (SP) using base classifier NC for applying different distance measures and m=1.1

Table 3. Maximum overall accuracy for H3 and H4 using NC as a base classifier for the combination of distance measures and γ for different values of λ where m=1.1

	DA(H3)			DA(H4)		
λ	γ	Overall Accuracy (OA)	Distance Measures	γ	Overall Accuracy (OA)	Distance Measures
0.2	0.9	0.83	Cosine	0.9	1.68	Chessboard
0.3	0.8	15.1	Chessboard	0.9	1.52	Chessboard
0.4	0.7	34.24	Mean Absolute Difference	0.9	2.72	Chessboard
0.5	0.9	62.70	Chessboard	0.8	15.63	Chessboard
0.6	0.8	65.93	Canberra	0.9	35.50	Mean Absolute Difference
0.7	0.9	73.61	Bray Curtis	0.9	61.11	Chessboard
0.8	0.7	77.08	Canberra	0.7	73.27	Mean Absolute Difference
0.9	0.9	82.16	Mean Absolute Difference	0.9	77.99	Canberra

Table 4. Maximum overall accuracy for SP using NC as a base classifier for the combination of distance measures and γ for different values of λ where m=1.1

	SP		
λ	β	Overall Accuracy (OA)	Distance Measures
0.2	9	13.78	Normalized Square Euclidean
0.3	9	20.53	Normalized Square Euclidean
0.4	9	47.29	Mean Absolute Difference
0.5	9	49.44	Canberra
0.6	8	67.95	Chessboard
0.7	7	69.21	Chessboard
0.8	8	70.55	Mean Absolute Difference
0.9	9	73.46	Bray-Curtis

Table 5. Maximum overall accuracy of H1, H2, H3, H4, and Smoothing Prior (SP) using base classifier NC for various distance measures and parameters (λ, γ, and β) where 'm'=1.1

Maximum Overall Accuracy	Bray Curtis	Canberra	Chessboard	Correlation	Cosine	Euclidean	Manhattan	Mean Absolute Difference	Median Absolute Difference	Normalized Square Euclidean
H1 (λ/ γ)	83.22 0.4/0.7	83.99 0.9/0.2	80.56 0.8/0.3	68.68 0.7/0.1	73.83 0.2/0.6	25.5 0.8/0.3	38.22 0.2/0.2	84.93 0.2/0.8	80.02 0.4/0.2	77.42 0.8/0.6
H2 (λ/ γ)	79.58 0.9/0.8	74.98 0.9/0.9	74.40 0.9/0.8	56.18 0.9/0.9	64.32 0.9/0.8	16.48 0.9/0.9	24.73 0.9/0.9	78.41 0.9/0.8	66.59 0.9/0.9	68.94 0.9/0.8
H3 (λ/ γ)	80.46 0.9/0.8	79.73 0.9/0.9	76.75 0.9/0.8	60.13 0.9/0.9	69.38 0.9/0.8	16.69 0.9/0.8	14.55 0.9/0.8	82.16 0.9/0.9	74.38 0.9/0.8	74.23 0.9/0.8
H4 (λ/ γ)	77.24 0.9/0.8	77.99 0.9/0.9	75.40 0.9/0.9	56.62 0.9/0.9	67.11 0.9/0.9	16.17 0.9/0.8	18.15 0.9/0.8	75.83 0.9/0.9	70.44 0.9/0.9	70.02 0.9/0.9
SP (λ/ β)	73.46 0.9/9	71.45 0.9/9	70.76 0.9/7	55.79 0.9/4	63.73 0.8/4	15.82 0.8/9	19.82 0.8/9	71.96 0.9/8	60.99 0.8/9	62.81 0.8/6

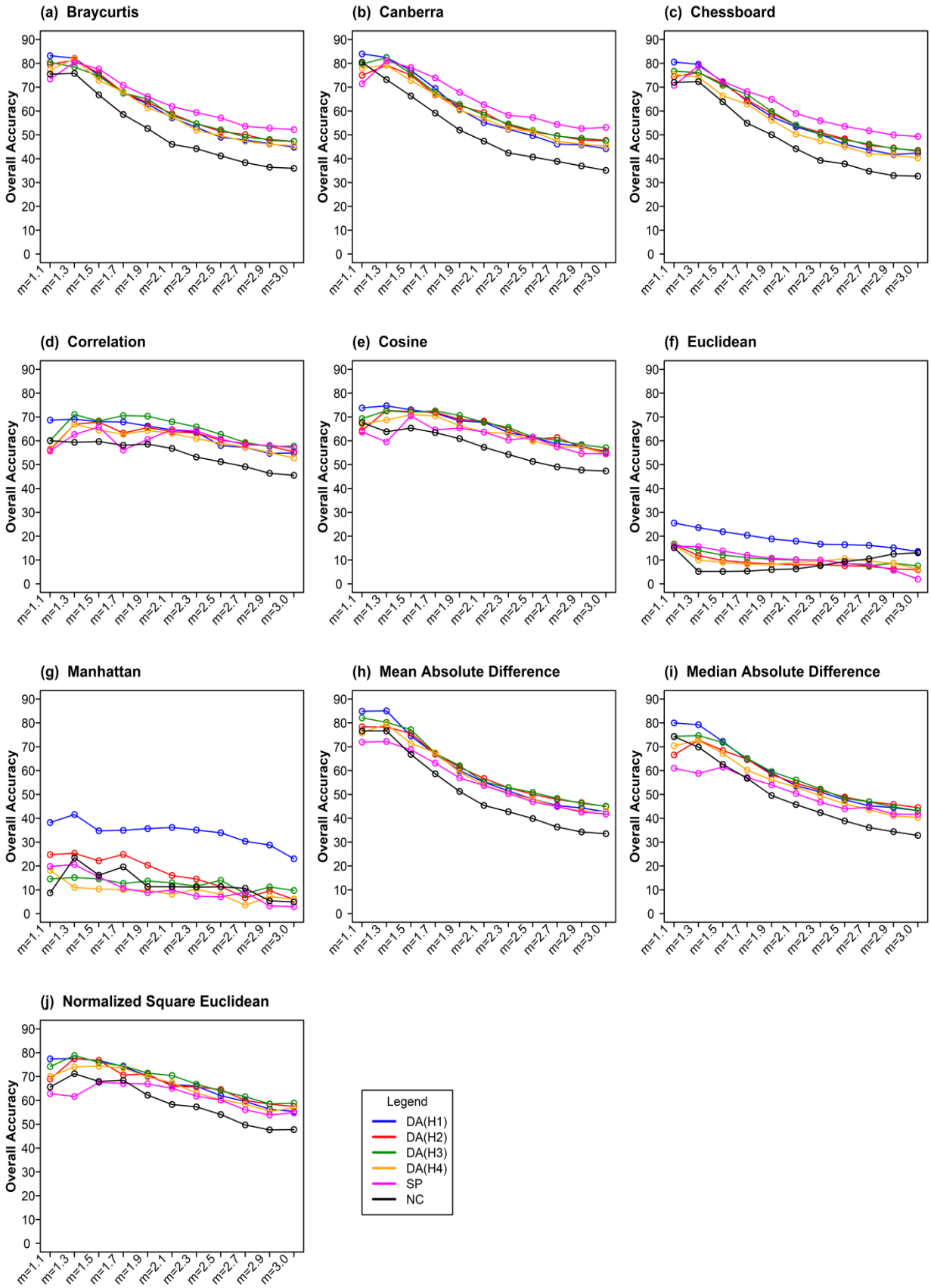

Figure 6. Comparison of Overall Accuracy in Discontinuity Adaptive Prior (DA) (H1, H2, H3, H4), Smoothing Prior (SP) and NC respectively for different m(1.1-3.0) and distance measures (a) Bray Curtis (b) Canberra (c) Chessboard (d) Correlation (e) Cosine (f) Euclidean (g) Manhattan (h) Mean Absolute Difference (i) Median Absolute Difference (j) Normalized Square Euclidean

Table 6. Highest OA occurred for NC and NC-based MRF models for different m value and distance measures

	DA(H1)		DA(H2)		DA(H3)		DA(H4)		SP		NC	
	OA	m	OA	m	OA	m	OA	m	OA	m	OA	m
Bray-Curtis	83.22	1.1	81.37	1.3	80.46	1.1	82.04	1.3	80.44	1.3	75.82	1.1
Canberra	83.99	1.1	79.25	1.3	82.37	1.3	79.30	1.3	81.08	1.3	80.48	1.1
Chessboard	80.56	1.1	76.14	1.3	76.75	1.1	75.4	1.1	79.01	1.1	72.34	1.3
Correlation	69.07	1.3	67.91	1.5	71.00	1.3	67.03	1.3	65.85	1.3	60.03	1.1
Cosine	74.68	1.3	72.80	1.3	72.57	1.3	70.98	1.5	70.46	1.5	67.65	1.1
Euclidean	25.50	1.1	16.48	1.1	16.69	1.1	16.17	1.1	15.82	1.1	15.18	1.1
Manhattan	41.56	1.3	25.31	1.3	15.14	1.3	18.15	1.1	20.60	1.1	23.48	1.3
Mean Absolute Difference	85.09	1.3	78.41	1.1	82.16	1.1	79.52	1.3	72.22	1.3	76.64	1.1
Median Absolute Difference	80.02	1.1	72.85	1.3	74.71	1.3	72.68	1.3	61.55	1.3	74.27	1.1
Normalized Square Euclidean	77.53	1.3	77.65	1.3	78.83	1.3	74.36	1.5	67.50	1.5	71.19	1.3

Table 7. The maximum overall accuracy of different algorithms using NC and NC based DA and SP algorithms concerning m and distance measures

Algorithm	m	Distance Measures	Overall Accuracy (%)
DA(H1)	1.3	Mean Absolute Difference	85.09
DA(H2)	1.3	Bray-Curtis	81.37
DA(H3)	1.3	Canberra	82.53
DA(H4)	1.3	Bray-Curtis	82.04
SP	1.3	Canberra	81.08
NC	1.1	Canberra	80.48

6. Conclusion

Traditional classification methods did not yield information on noisy and nearby pixels. On the other hand, the MRF model method takes care of the noisy and nearby pixels. This paper used Various MRF models, such as SP and DA (H1, H2, H3, and H4), to optimize the approach while considering distance measures and different parameters λ, β, γ, and m). The NC classifier as a base for SP and DA (H1, H2, H3, and H4) compares various distance measures and parameters to achieve the best technique. With $\gamma = 0.8$, $\delta = 10^4$, $m = 1.3$, and $\lambda = 0.2$, DA (H1) provided the highest overall accuracy of 85.09 % for Mean Absolute Difference distance measures. This study will also help find the optimized parameters (γ, β, m, and λ) and distance measures for MRF models (SP and DA) by applying NC as a base classifier to obtain the highest accuracy and classify the images perfectly.

Acknowledgment

The authors would like to express their sincere gratitude to the Department of Mining Engineering, Indian Institute of Technology (Indian School of Mines), Dhanbad for their help and support, and also to the Indian Institute of Remote Sensing Dehradun for their kind co-operation during the course of this study.

References

Agarwal S., C. Burgess and K. Crammer (2009). Advances in ranking. In *Workshop, Twenty-Third Annual Conference on Neural Information Processing Systems, Whistler, BC.*

Baccour L. and RI John (2014). Experimental analysis of crisp similarity and distance measures. In *2014 6th*

International Conference of Soft Computing and Pattern Recognition (SoCPaR) (pp. 96-100). IEEE.

Bezdek J. C., R. Ehrlich and W. Full (1984). FCM: The fuzzy c-means clustering algorithm. *Computers & geosciences*, *10*(2-3), 191-203.

Binaghi E. and A. Rampini (1993). Fuzzy decision making in the classification of multisource remote sensing data. *Optical Engineering*, *32*(6), 1193-1204.

Binaghi E., PA Brivio, P. Ghezzi and A. Rampini (1999). A fuzzy set-based accuracy assessment of soft classification. *Pattern recognition letters*, *20*(9), 935-948.

Bray J. R. and JT Curtis (1957). An ordination of the upland forest communities of southern Wisconsin. *Ecological monographs*, *27*(4), 326-349.

Davé R. N. and R. Krishnapuram (1997). Robust clustering methods: a unified view. *IEEE Transactions on fuzzy systems*, *5*(2), 270-293.

Fisher P. (1997). The pixel: a snare and a delusion. *International Journal of Remote Sensing*, *18*(3), 679-685.

Geman S., & Geman D. (1984). Stochastic relaxation, Gibbs distributions, and the Bayesian restoration of images. *IEEE Transactions on pattern analysis and machine intelligence*, (6), 721-741.

Hasnat A., S. Halder, D. Bhattacharjee, M. Nasipuri and DK Basu (2013). Comparative study of distance metrics for finding skin color similarity of two color facial images. *ACER: New Taipei City, Taiwan*, 99-108.

Krishnapuram R. and JM Keller (1993). A possibilistic approach to clustering. *IEEE transactions on fuzzy systems*, *1*(2), 98-110.

Li S. Z. (1995). On discontinuity-adaptive smoothness priors in computer vision. *IEEE Transactions on Pattern Analysis and Machine Intelligence*, *17*(6), 576-586.

Rawat A., D. Kumar, RS Chatterjee and H. Kumar (2022a). A GIS-based liquefaction susceptibility mapping utilising the morphotectonic analysis to highlight potential hazard zones in the East Ganga plain. Environmental Earth Sciences, 81(13), 1-16.

Rawat A., D. Kumar, RS Chatterjee and H. Kumar (2022b). Reconstruction of liquefaction damage scenario in Northern Bihar during 1934 and 1988 earthquake using geospatial methods. Geomatics, Natural Hazards and Risk, 13(1), 2560-2578.

Saha A., VGK Villuri and A. Bhardwaj (2022). Development and Assessment of GIS-Based Landslide Susceptibility Mapping Models Using ANN, Fuzzy-AHP, and MCDA in Darjeeling Himalayas, West Bengal, India. Land, 11(10), 1711.

Scollar I., B. Weidner and TS Huang (1984). Image enhancement using the median and the interquartile distance. Computer vision, graphics, and image processing, 25(2), 236-251.

Suman S., D. Kumar and A. Kumar (2022). Study the Effect of the MRF Model on Fuzzy c Means Classifiers with Different Parameters and Distance Measures. Journal of the Indian Society of Remote Sensing, 1-13.

Senoussaoui M., P. Kenny, T. Stafylakis and P. Dumouchel (2013). A study of the cosine distance-based mean shift for telephone speech diarization. IEEE/ACM Transactions on Audio, Speech, and Language Processing, 22(1), 217-227.

Singh P. P. and RD Garg (2017). On sphering the high resolution satellite image using fixed point based ICA approach. In Proceedings of International Conference on Computer Vision and Image Processing (pp. 411-419). Springer, Singapore.

Smits P. C. and SG Dellepiane (1997, August). Discontinuity adaptive MRF model for remote sensing image analysis. In IGARSS'97. 1997 IEEE International Geoscience and Remote Sensing Symposium Proceedings. Remote Sensing-A Scientific Vision for Sustainable Development (Vol. 2, pp. 907-909). IEEE.

Solberg AHS, T Taxt and AK Jain (1996), A Markov Random Field Model for classification of multisource satellite imagery in IEEE Transcation on Geoscience and Remote Sensing Vol. 34, PP. 100-113.

Székely G. J., ML Rizzo and NK Bakirov (2007). Measuring and testing dependence by correlation of distances. The annals of statistics, 35(6), 2769-2794.

Tso B. and RC Olsen (2005). A contextual classification scheme based on MRF model with improved parameter estimation and multiscale fuzzy line process. Remote Sensing of Environment, 97(1), 127-136.

Vassiliadis S., EA Hakkennes, JSSM Wong and GG Pechanek (1998, August). The sum-absolute-difference motion estimation accelerator. In Proceedings. 24th EUROMICRO Conference (Cat. No. 98EX204) (Vol. 2, pp. 559-566). IEEE.

Zhang B., S. Li, X. Jia, L. Gao and M Peng (2011). Adaptive Markov random field approach for classification of hyperspectral imagery. IEEE Geoscience and Remote Sensing Letters, 8(5), 973-977.